

**IDEA StatiCa Member**

**WP1-2: Comparison of the Buckling Resistance of I-shaped cross-sections**

*Project Partner:*

IDEA StatiCa

**Final Report**

*Report Author*

ANDREAS MÜLLER M.Sc.

*Responsible Investigator*

Prof. Dr. techn. ANDREAS TARAS

Chair of Steel and Composite Structures

Institute of Structural Engineering (IBK)

ETH Zurich

## Table of contents

1. Introduction.....	3
2. Model Description.....	3
3. Choice and Validation of the Abaqus model.....	5
4. Choice of imperfections.....	8
4.1. Local imperfections .....	8
4.2. Global Imperfections.....	9
5. Comparisons and Recommendations.....	14
5.1. Comparison of the LBA Results:.....	14
5.2. Comparison of the GMNIA Results: .....	20
6. Choice of eigenmode shapes for interactive cases of global + local buckling.....	22
7. Conclusions.....	26
8. Literature and References .....	27

## 1. Introduction

### Objective and Scope

The objective of this report is the verification of the LBA (linear buckling analysis) and GMNIA (**g**eometrically and **m**aterial **n**onlinear **a**nalysis with **i**mperfections) module of the IDEA StatiCa Member software application version 21.0. The resulting resistances from IDEA StatiCa Member are compared with equivalent Abaqus CAE 2019 [1] simulations. For the recommendation of local and global imperfection assumptions, additional Abaqus simulations were performed. Therefore, the selected imperfections were chosen according to the specifications of EN 1993-1-1 [2], prEN 1993-1-1 [3] and EN 1993-1-5 [4]. Further considerations regarding the choice of eigenmode shapes for interactive cases of global + local buckling were carried out with the aim of creating practice-oriented recommendations. Finally, recommendations are developed for practical design using IDEA StatiCa Member.

## 2. Model Description

A general FEM-model overview is shown in Fig. 1 and Fig. 2. The IDEA StatiCa Member model consists of three basic parts, the analysed member itself and two additional related members with a far higher stiffness than the actual member. This provides an exclusive failure in the member without the influence of the top and bottom edge boundaries. The setting for the generation of the mesh "Number of elements on biggest member web or flange" was adjusted from the default value of 20 to a higher value of 30, in order to match the mesh of the ABAQUS models. All additional values within the "Code and calculation settings" were not changed. The loads were applied through the boundaries at the top and bottom plate as shown in Fig. 1 in order to create different  $N$ - $M$  load interactions. Butt welds were selected to achieve fixed boundary conditions of plates of I-shaped sections to the related members and to avoid any failure of welds prior to failure of the sections.

An equivalent Abaqus comparison model is shown in Fig. 2, where the use was made of three-dimensional shell elements of type S4R. The boundary conditions and additional loads were applied through reference points (RF-Points) at the top and the bottom, each connected through an MPC-Beam (multiple point constraint) formulation to associated node sets on the outer extremities (red dotted edges). The edges of the I-shaped sections were fixed to these MPC-Beams. The web and the flanges were discretized into 30 and 20 elements, respectively. A thorough look at additional possible model solutions from literature – regarding its advantages and disadvantages – is taken in Section 3, followed by a subsequent modelling choice and validation.

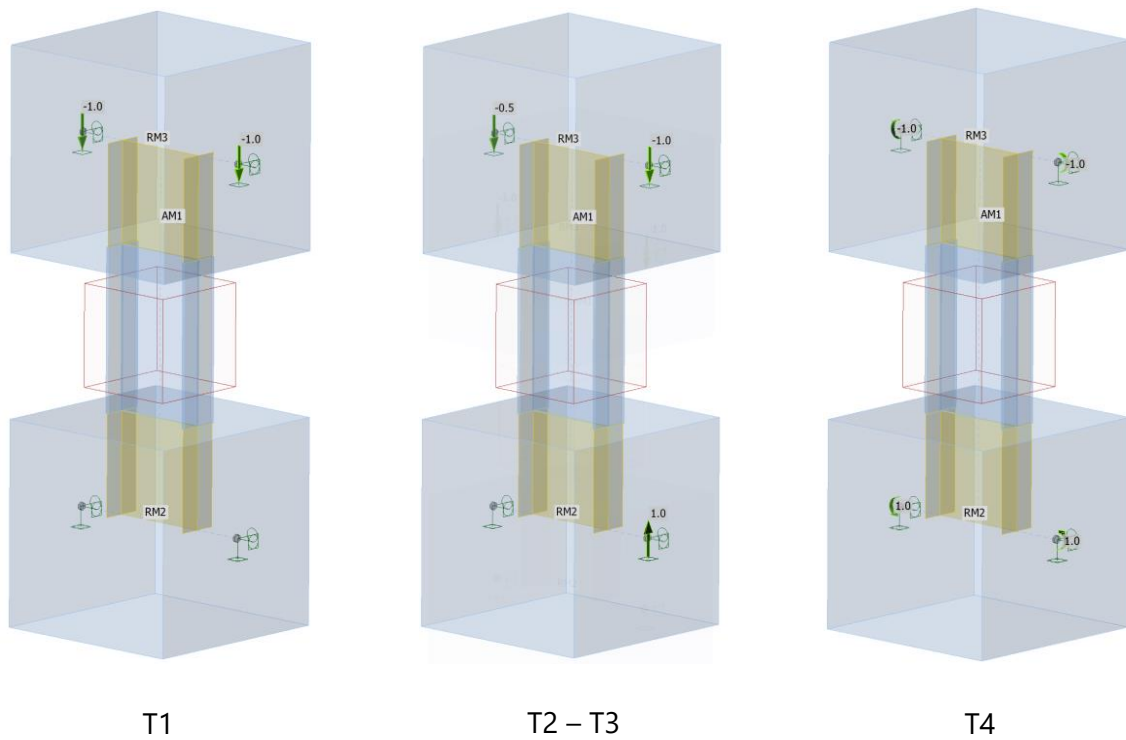


Figure 1: IDEA StatiCa Member transparent model for different load situations T1, T2-T3, T4

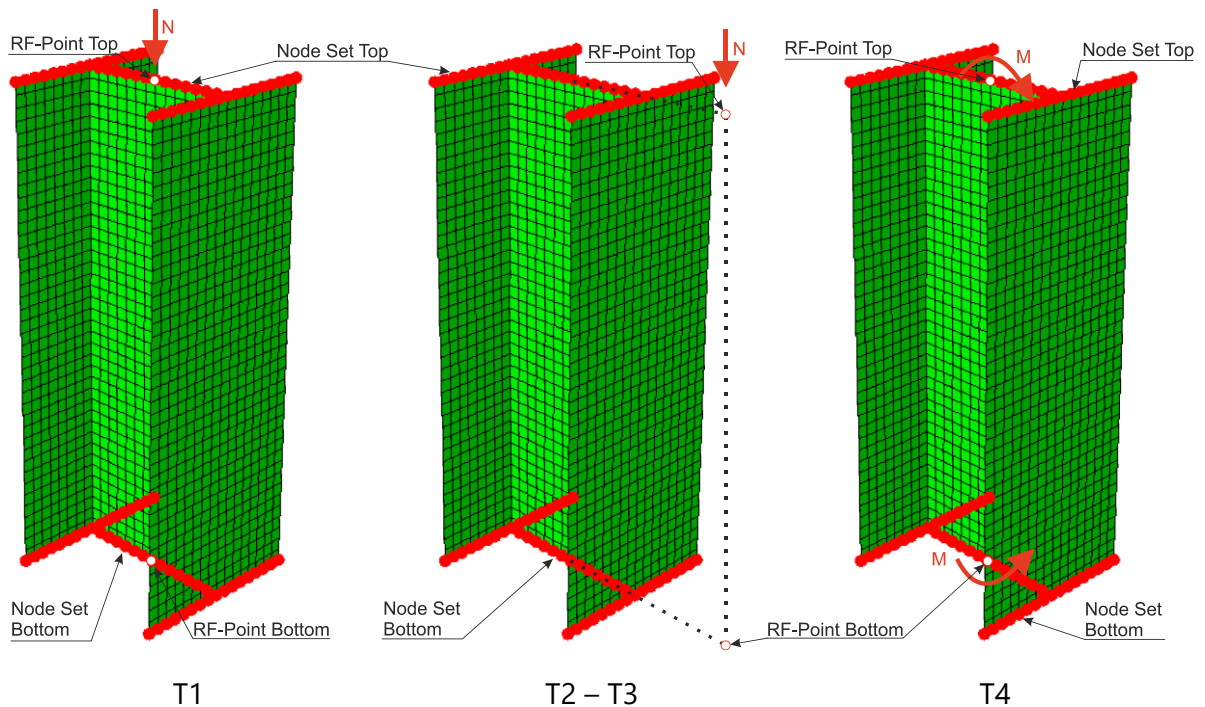


Figure 2: General Abaqus FE-Models for different load situations T1, T2-T3, T4

In total 56 models (see Tab. 1) were compared, regarding different load combinations of normal force and moment (T1 to T4), imperfection amplitudes and cross-section slenderness. The chosen steel grade of S355 and the member length of the considered cross-sections with 800 mm was set constant throughout the investigations.

Table 1: Parameter overview

	HEA300	HEA800	IPE300	IPE500
Considered Cross-Sections	HEA300	HEA800	IPE300	IPE500
Imperfection amplitude	$d/200$ $d/400$	$d/200$ $d/400$	$d/200$ $d/400$	$d/200$ $d/400$
Load combinations	<u>T1</u> : $N$		<u>T1</u> : $N$	
	$N$ - $M$ : <u>T2<sub>y</sub></u> : $e_y = 60\text{mm}$ ; <u>T2<sub>z</sub></u> : $e_z = 60\text{mm}$ <u>T3<sub>y</sub></u> : $e_y = 300\text{mm}$ ; <u>T3<sub>z</sub></u> : $e_z = 300\text{mm}$		$N$ - $M$ : <u>T2<sub>y</sub></u> : $e_y = 60\text{mm}$ ; <u>T2<sub>z</sub></u> : $e_z = 60\text{mm}$ <u>T3</u> : $e_y = 300\text{mm}$ ; <u>T2<sub>z</sub></u> : $e_z = 300\text{mm}$	
	<u>T4<sub>y</sub></u> : $M$	<u>T4<sub>z</sub></u> : $M$	<u>T4<sub>y</sub></u> : $M$	<u>T4<sub>z</sub></u> : $M$

### 3. Choice and validation of the Abaqus model

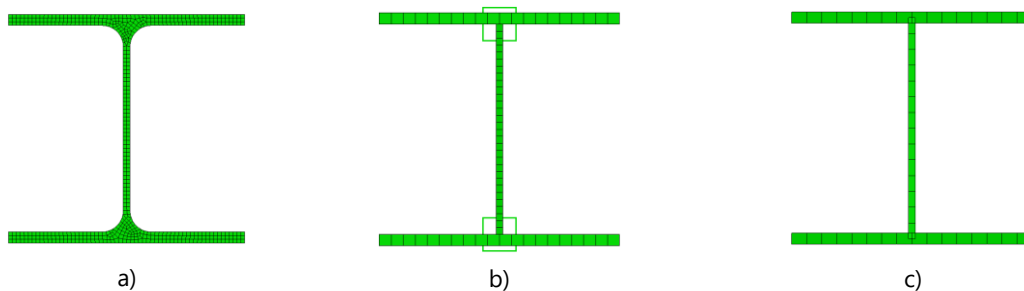


Figure 3: Common model approaches for I- and H-shaped profiles a) Solid-model; b) Shell-beam-model; c) Shell-model

Three common models for I- and H-shaped profiles are summarized in Fig. 3, including a) solid-model; b) shell-beam-model; c) shell-model. Solid models (see Fig. 3 a)) can lead to a realistic geometry approximation, including the influence of the fillets between the web and the flanges.

Nevertheless, requiring the implementation of the whole cross-section geometry, the calculation process can become computationally time-consuming, leading to necessary simplifications within the models.

A more simplified model is shown in Fig. 3 b), where the flanges and the web are modeled with shell elements, without a surface interception but with additional beam elements as square hollow sections of variable depth and wall thickness at the top and the bottom of the web. The beam elements are designed in such a way that they have the same area  $A$  and torsional moment of inertia  $I_T$  as the missing fillets between the web and flanges. This modelling approach was also successfully used and verified in [5].

One further approach is the use of a shell-model with three plates representing the web and the flanges, which are intercepting in the centerline; see Fig. 3 c). Therefore, the fillets are not modelled explicitly but are approximated by the overlap between the web and the flanges. Following this model assumption not all cross-section values can be taken into account precisely for hot rolled I-shaped sections; welded profiles are mostly excluded from this. In some cases, especially the torsional moment of inertia  $I_T$  can deviate, depending on the selected profile series, around 30% [6]. This can lead, in accordance to the observed problem, to lower capacity values e.g. in the case of lateral-torsional buckling (LTB). However, for local instability problems, which were investigated throughout this report, members of shorter span are primarily not prone to LTB effects and therefore the above-mentioned modelling shortfall is negligible. For this reason, model c offers several strategical and numerical advantages e.g. higher computational efficiency and higher model homogeneity as applicable for both hot rolled and welded I-shaped profiles.

A preliminary investigation between the above described Abaqus models (Fig. 3) and Idea StatiCa Member was conducted to point out the differences and underline the choice of the used Abaqus model for the later procedure, see Section 5. Therefore, an HEA300 profile with a length of 800 mm and the steel grade S355 was selected and loaded with a normal force acting in the center of gravity. In a first step, a linear bifurcation analysis (LBA) was performed in Idea StatiCa Member to find an optimal discretization density or in general an optimal number of elements, which is denoted in the program intern settings as a variable input value "Number of elements on biggest member web or flange". With constantly increasing number of elements within the cross-section the computed eigenvalues start to converge towards a fixed cross-section dependent value. This convergence was obtained for a number of approximately 30 elements within the bigger member, which appear to be the flange for the used HEA300 profile (see Tab. 2, Idea StatiCa Member benchmark model highlighted in green). The LBA benchmark results are then compared with the investigated Abaqus models a, b, and c. Table 2 displays the results and its additional deviations in percent for the three first eigenmodes. The highest deviations, always using the model of Idea StatiCa Member as a benchmark, results for model a (solid-model) and model b (shell-beam-model). The lowest difference occurs for Abaqus model c, since its modelling approach corresponds to the configuration of the model in Idea StatiCa Member. In contrast, the GMNIA results (see Tab. 3) do not show any significant differences in comparison, with model c being the most accurate within this analysis as well.

Table 2: LBA Results for different model approaches for an HEA300 profile

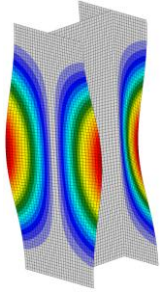
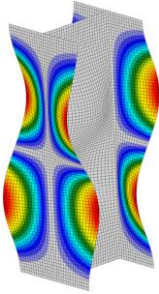
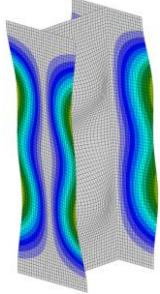
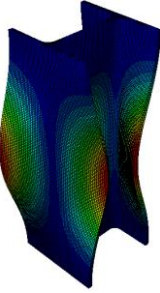
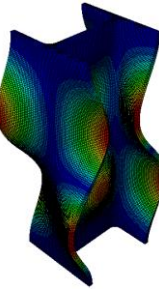
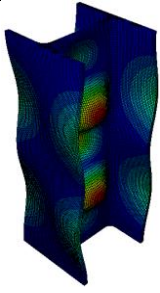
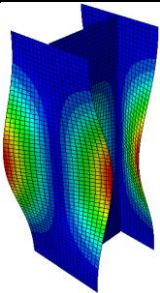
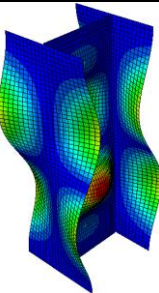
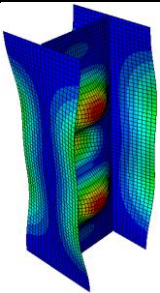
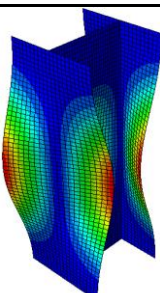
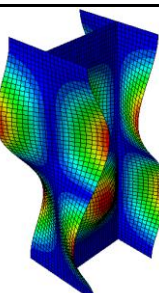
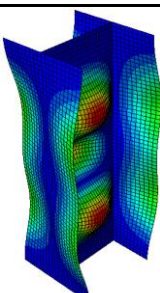
LBA	Eigenvalue (kN)		
	EV1	EV2	EV3
IDEA StatiCa			
8*	10720.00	11920.00	13720.00
20*	10560.00	11600.00	13160.00
30* (picked benchmark model)	10510.00	11546.20	13087.00
40*	10510.00	11546.20	13080.00
Abaqus Model a)			
	12876.80 (+22.5%)	13783.20 (+19.40%)	15004.10 (+14.65%)
Abaqus Model b)			
	13981.50 (+33.0%)	14676.00 (+27.11%)	15501.90 (+18.45%)
Abaqus Model c) (picked Abaqus model)			
	10505.00 (-0.005%)	11585.30 (+0.34%)	13112.20 (+0.19%)
*Number of elements on biggest member web or flange			

Table 3: GMNIA Results for different model approaches for an HEA300 profile

GMNIA	Maximum Peak Load (kN)
IDEA StatiCa	3796.00
Abaqus Model a)	4017.00 (+5.82%)
Abaqus Model b)	4019.00 (+5.87%)
Abaqus Model c)	3814.40 (+0.48%)

Based on these results, it is most appropriate to use model c for further investigations, following in Section 5, as the focus is exclusively laid on the comparison between the simulation results of finite element models and not e.g. a model calibration.

A general validation against literature was carried out for model b (shell-beam-model) as a preliminary step to verify overall modelling correctness. Therefore different N-M interactions were taken into account to calculate a range of critical bifurcation loads (combined lateral-torsional-buckling- and flexural-buckling loads), normalized by the plastic cross-section resistance. The comparison with analytical solutions from *Trahair* [7] showed sufficient results. In addition, GMNIA calculations for the flexural buckling case about the weak axis were carried out for different I and H sections. A comparison with the originally developed ECCS curves for flexural buckling (Beer and Schulz [8]) showed a good agreement of the performed GMNIA calculations with published and accepted solutions. Further details on an equivalent model validation can be taken from [5].

## 4. Choice of imperfections

### 4.1. Local imperfections

According to EN 1993-1-5, Annex C [4] the magnitude of local imperfections for the analysis of plate buckling may be assumed with a value of  $e_0 = d/200$ , where  $d$  is the height of an individual field. In the considered case of hot-rolled I-shaped sections,  $d$  was assumed to be the height of the web without the geometric consideration of the fillets. In addition, various parameters such as the steel grade (S235, S355, S460), different profile geometries (HEA300, HEA800, IPE300, IPE500, IPE600) and imperfection amplitudes ( $d/200$ ,  $d/300$ ,  $d/400$ ) were taken into account to perform further GMNIA calculations. This was done to find a suitable imperfection amplitude that represents the design curve for local buckling ("Winter curve") of EN 1993-1-5 [4] in an appropriate manner. The variation of profiles and steel grades was primarily done to estimate a wider slenderness range. A summary of the numerical calculations can be seen in Fig. 4. The  $y$ -axis is represented by a buckling knock down factor  $\rho$ , which is defined as the estimated local load bearing capacity from GMNIA simulations, normalized by the plastic cross-sectional resistance and calculated from the nominal value of  $f_y \cdot A$ , where  $A$  is the cross-section area of the assumed Abaqus shell model from Fig. 3 c). The local slenderness  $\bar{\lambda}_\rho$  is



applied over the  $x$ -axis and defined as the square root of the plastic cross-section resistance divided by the critical local buckling load estimated from a linear buckling analysis (LBA).

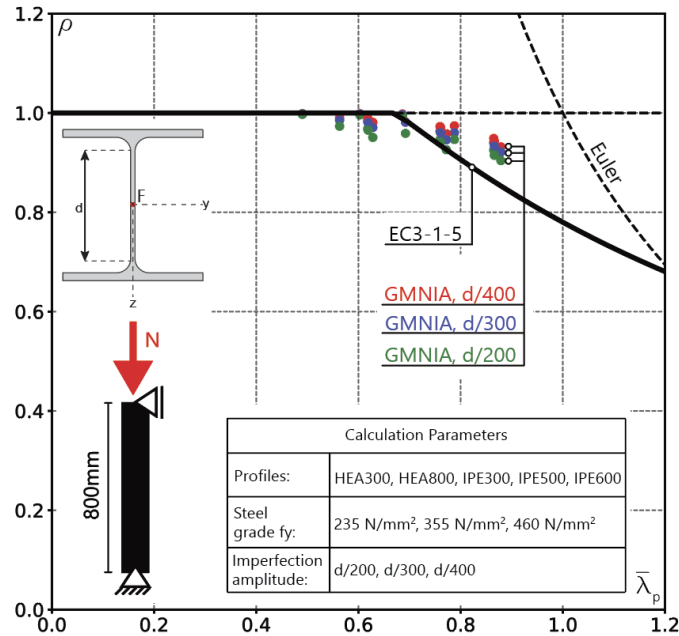


Figure 4: GMNIA simulations and comparison with code provision of EN 1993-1-5 [4]

The red, blue and green dots represent the results from the performed GMNIA simulations, where each colour represents a different imperfection amplitude along a visible slenderness range. All calculations show a relatively small scatter, coming to lie near the local buckling curve of EN 1993-1-5 [4]. Based on these results, the imperfection amplitude of  $d/200$  specified in [4] is still recommended for practical use.

#### 4.2. Global Imperfections

The general preselection of the initial imperfection magnitude depends on different factors like: (i) the type of analysis according to the considered cross-section failure linked to the cross-section class, (ii) the type of imperfection considered for further calculations i.e. geometric imperfections only or equivalent imperfections including a geometric bow imperfection and additional residual stresses, (iii) the benchmark resistance in term of plastic or elastic calculation which specify the choice of imperfection. The latter corresponds to the global buckling concept of EN 1993-1-1 [2], where a cross-section dependent imperfection factor  $\alpha$  takes both into account.

According to EN 1993-1-1 [2] and prEN1993-1-1 [3] the bow imperfection amplitude,  $e_0$ , can be determined using two approaches, considering either a tabulated length proportional value or a slenderness-based formulation based on the elastic critical buckling modes. According to EN 1993-1-1, Table 5.1 [2]  $e_0$  is the ratio between the member length and a value that depends on the global buckling curve ( $a_0$ ,  $a$ ,  $b$ ,  $c$ ,  $d$ ) and the analysis type: elastic or plastic. A summary of GMNIA calculation is presented in Fig. 5, Fig. 6 and Fig. 7, each representing the results for an HEA300 profile of varying length and buckling about both axes  $z$ - $z$  and  $y$ - $y$ , respectively.

In the current draft of prEN1993-1-1 [3], a modified formulation for the determination of the length affine imperfection  $e_0$  is presented (see Eq. 1). Where  $\alpha$  is the imperfection factor, depending on the relevant buckling curve,  $\varepsilon$  the material parameter considering the steel grade,  $\beta$  the reference bow imperfection and  $L$  the total member length. The choice of the reference bow imperfection on the one hand depends on the design method (elastic or plastic) and on the other hand the relevant buckling axis ( $y$ - $y$  or  $z$ - $z$ ). The associated numerical simulations can be seen in Fig. 6.

$$e_0 = \frac{\alpha}{\varepsilon} \cdot \beta \cdot L \quad (1)$$

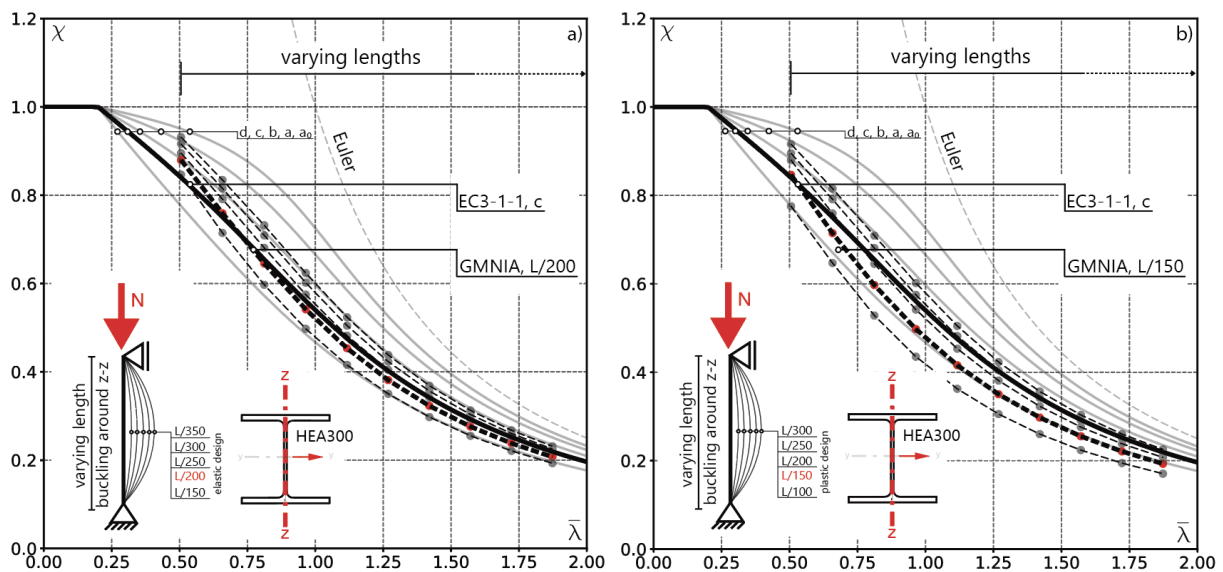
Table 4: Reference bow imperfection  $\beta$  [3]

Buckling about axis	Elastic design	Plastic design
$y$ - $y$	1/110	1/75
$z$ - $z$	1/200	1/68

The back-calculation of slenderness-based equivalent bow imperfections, in both EN 1993-1-1 [2] and prEN 1993-1-1 [3], is provided by Eq. 2.

$$e_0 = \alpha \cdot (\bar{\lambda} - 0.2) \frac{M_{Rk}}{N_{Rk}} = \alpha \cdot (\bar{\lambda} - 0.2) \frac{W}{A} \quad (2)$$

Where  $e_0$  is the target imperfection,  $\alpha$  the imperfection factor for the relevant buckling curve,  $\bar{\lambda}$  the member relative slenderness,  $M_{Rk}$  the characteristic moment resistance of the critical cross-section and  $N_{Rk}$  the characteristic axial resistance of the cross-section. The imperfection amplitudes calculated this way result in smaller deflections and thus resistances that are closer to the buckling curves. Fig. 7 gives an overview of GMNIA calculations based on the elastic (Fig. 7 a, b) and plastic (Fig. 7 c, d) resistance.



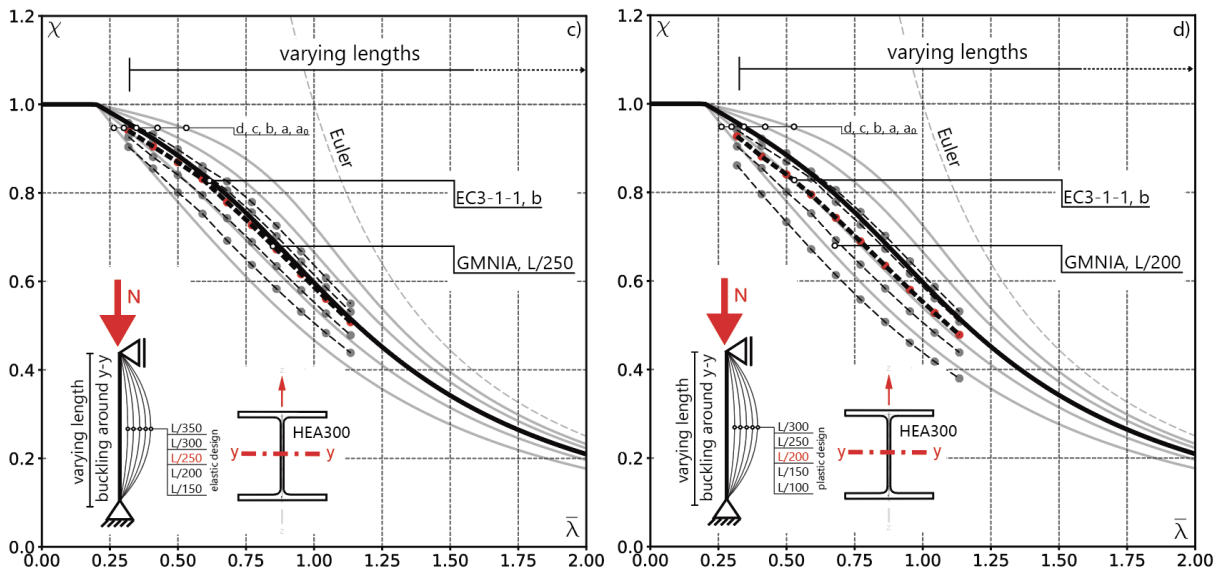
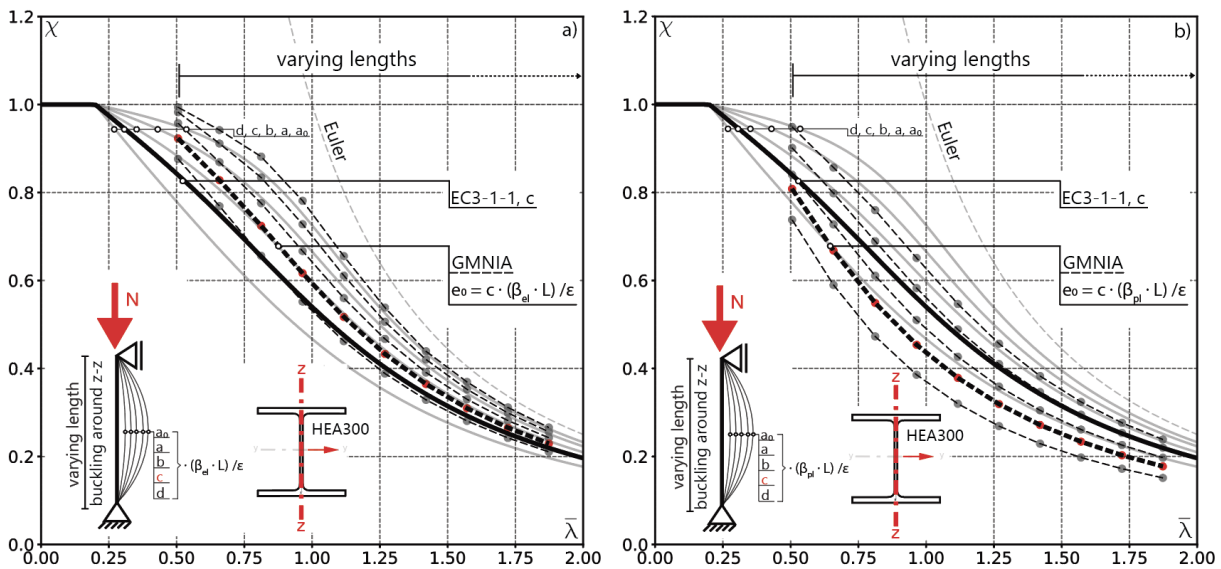


Figure 5: Length affine [2] GMNIA calculations for an HEA300 profile and comparison with code provision of EN 1993-1-1 [2] a) buckling around z-z elastic design; b) buckling around z-z plastic design, c) buckling around y-y elastic design, d) buckling around y-y plastic design



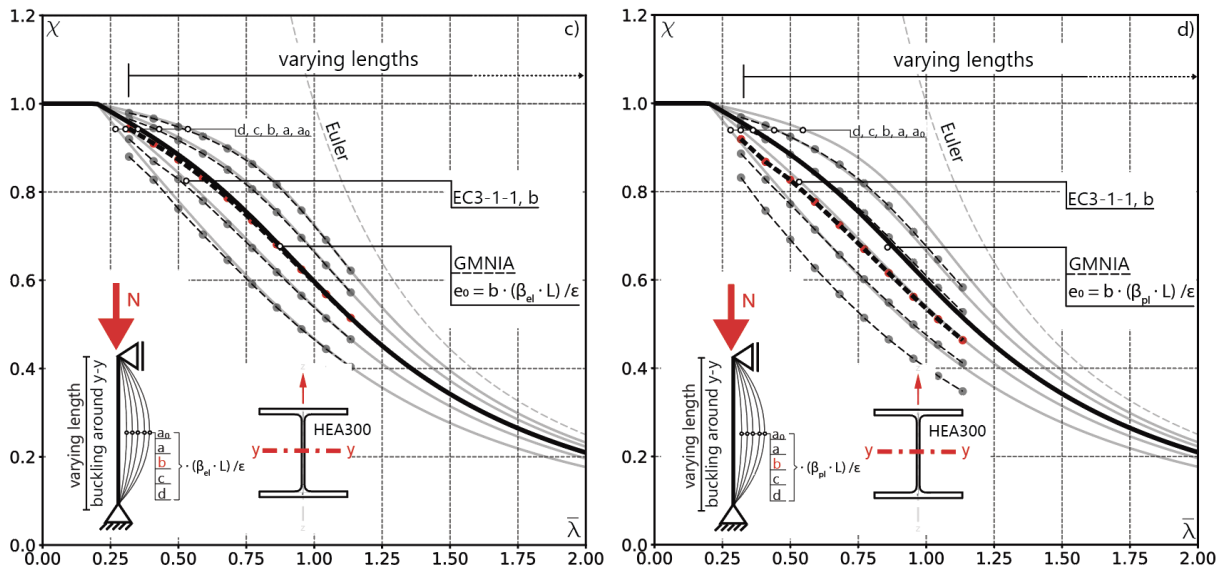
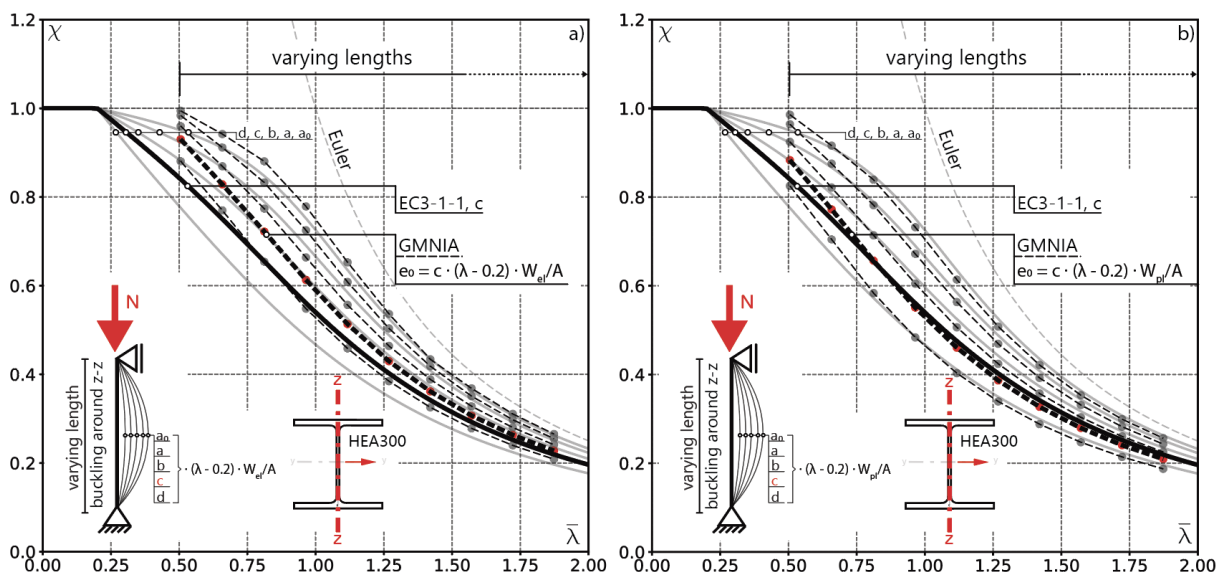


Figure 6: Length affine [3] GMNIA calculations for an HEA300 profile and comparison with code provision of EN 1993-1-1 [2] a) buckling around z-z elastic design; b) buckling around z-z plastic design, c) buckling around y-y elastic design, d) buckling around y-y plastic design

The basic layout of Fig. 5, 6 and 7 is in all cases the same, where the  $y$ -axis is represented by the global buckling reduction factor  $\chi$ , defined by the estimated global resistance and divided through the nominal plastic cross-section resistance  $N_{pl}$ . Again, as in the case of the assessment of local imperfections, the calculated value of  $N_{pl} = f_y \cdot A$  is based on the nominal values of  $f_y$  and  $A$  being the cross-section area of the assumed Abaqus shell model from Fig. 3 c). The determined reduction factors are plotted over a normalized global slenderness  $\bar{\lambda}$  along the  $x$ -axis. Therefore the global slenderness was calculated from the square root of the plastic cross-section resistance divided by the critical buckling load, see Eq. 3.

$$\bar{\lambda} = \sqrt{\frac{N_{pl}}{N_{cr,LBA}}} \quad (3)$$



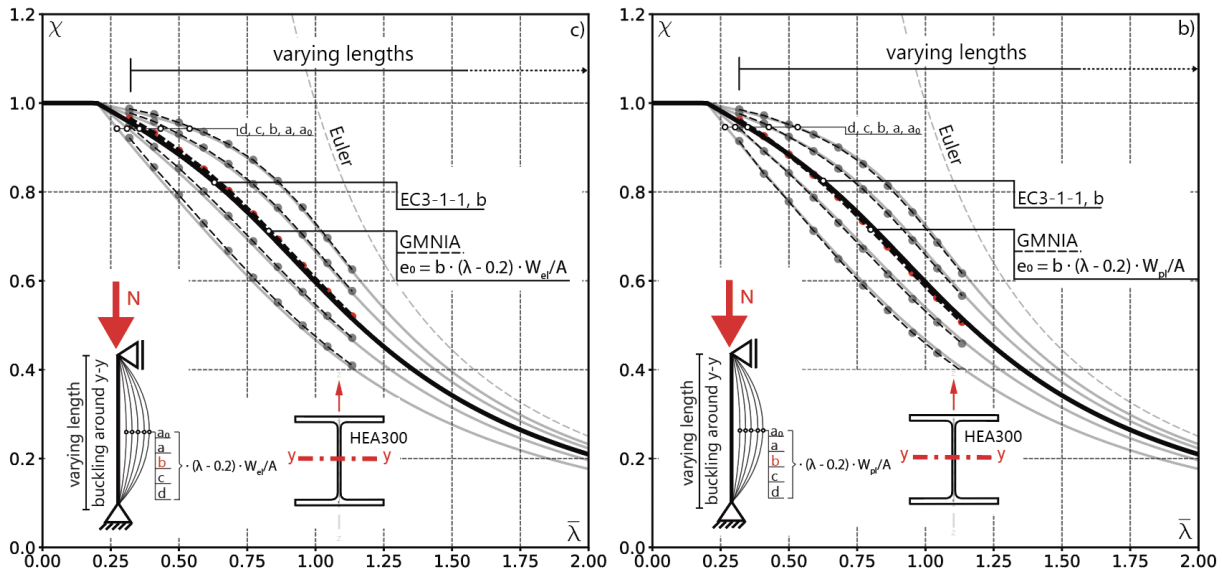


Figure 7: Slenderness affine [2] GMNIA calculations for an HEA300 profile and comparison with code provision of EN 1993-1-1 [2] a) buckling around z-z elastic design; b) buckling around z-z plastic design, c) buckling around y-y elastic design, d) buckling around y-y plastic design

In the case of the current length affine formulation of the imperfection amplitude according to EN 1993-1-1 [2], the elastic design approach leads to estimated numerical results, which follow closely the significant buckling curve c for buckling around z-z axis and buckling curve b for buckling around y-y axis (Fig. 5 a) and c)). A slightly higher deviation and therefore a more conservative assessment is detected throughout the whole slenderness range for buckling around z-z and y-y axis in the case of plastic design, comparing the results with the relevant buckling curve c and b, respectively (Fig. 5 b) and d)).

The same applies in the case of the new length affine formulation for the imperfection amplitude according to pEN1993-1-1 [3]. Even though the elastic design approach for buckling around z-z axis (Fig. 6 a)) produces results, which are more optimistic in the case of the considered HEA300 profile, the estimated results for buckling around y-y axis (Fig. 6 c)) are very accurate laying precisely on buckling curve b. The plastic design approach generally shows more conservative results in both cases for buckling around z-z and y-y axes (Fig. 6 b, d), respectively, where the resulting reduction factors always lie below the buckling curves.

The latter imperfection formulation (slenderness affine, Fig. 7) leads in the case of the elastic design approach to results that are too optimistic over the whole slenderness range for buckling around z-z axis. Although the results for buckling around y-y axis (elastic design) look very accurate, it is recommended to use in both buckling directions the slenderness affine imperfection amplitudes from the elastic design formulation since the results are slightly on the safe side below the global buckling curves (Fig. 7 b) and d)). In terms of practical usability, the length affine approach requires fewer computationally intensive steps – calculation of the slenderness, which requires the determination of the critical buckling load and the cross-section resistance – and is therefore simpler in its overall application.

## 5. Comparisons and Recommendations

### 5.1. Comparison of the LBA Results:

Table 5: LBA Results – HEA300

	Eigenvalue (EV)		
	EV1	EV2	EV3
<b>HEA300</b>			
<b>T1 in [kN]</b>			
IDEA StatiCa	10510.04	11546.19	13087.01
Abaqus	10505.00	11585.28	13112.20
Comparison	100%	99.70%	99.80%
<b>T2<sub>y</sub> in [kN]</b>			
IDEA StatiCa	8000.00	8500.00	11400.00
Abaqus	7983.80	8566.40	11485.40
Comparison	100.20%	99.20%	99.30%
<b>T2<sub>z</sub> in [kN]</b>			
IDEA StatiCa	7830.00	7860.00	8100.00
Abaqus	7832.41	7861.24	8126.86
Comparison	100.00%	100.00%	99.70%
<b>T3<sub>y</sub> in [kN]</b>			
IDEA StatiCa	3480.00	3720.00	5040.00
Abaqus	3497.31	3726.51	5089.76
Comparison	99.50%	99.80%	99.00%
<b>T3<sub>z</sub> in [kN]</b>			
IDEA StatiCa	2610.00	2640.00	2700.00
Abaqus	2628.59	2645.54	2705.85
Comparison	99.30%	99.80%	99.80%
<b>T4<sub>y</sub> in [kNm]</b>			
IDEA StatiCa	1477.00	1568.00	2136.00
Abaqus	1479.00	1571.11	2144.62
Comparison	99.90	99.80	99.60
<b>T4<sub>z</sub> in [kNm]</b>			
IDEA StatiCa	933.00	933.00	960.00
Abaqus	934.74	934.74	962.66
Comparison	99.80%	99.80%	99.70%

Table 6: LBA Results – HEA800

	Eigenvalue (EV)		
	EV1	EV2	EV3
<b><u>HEA800</u></b>			
<b>T1 in [kN]</b>			
IDEA StatiCa	17400.00	21200.00	35600.00
Abaqus	17375.90	21055.50	34710.50
Comparison	100.1%	100.7%	102.6%
<b>T2<sub>y</sub> in [kN]</b>			
IDEA StatiCa	17400.00	21150.00	35250.00
Abaqus	17343.00	20976.00	34416.40
Comparison	100.3%	100.8%	102.4%
<b>T2<sub>z</sub> in [kN]</b>			
IDEA StatiCa	17550.00	21300.00	35250.00
Abaqus	17360.650	21049.10	34692.00
Comparison	101.1%	101.2%	101.6%
<b>T3<sub>y</sub> in [kN]</b>			
IDEA StatiCa	16800.00	19800.00	30600.00
Abaqus	16573.60	19411.30	29979.80
Comparison	101.4%	102.0%	102.1%
<b>T3<sub>z</sub> in [kN]</b>			
IDEA StatiCa	16830.00	19350.00	19650.00
Abaqus	16567.60	18925.00	19222.50
Comparison	101.6%	102.2%	102.2%
<b>T4<sub>y</sub> in [kNm]</b>			
IDEA StatiCa	23160.00	24180.00	30480.00
Abaqus	23003.00	24087.10	30168.50
Comparison	100.7%	100.4%	101.0%
<b>T4<sub>z</sub> in [kNm]</b>			
IDEA StatiCa	6600.00	6660.00	6840.00
Abaqus	6571.23	6584.88	6755.00
Comparison	100.4%	101.1%	101.3%



Table 7: LBA Results – IPE300

	Eigenvalue (EV)		
	EV1	EV2	EV3
<b><u>IPE300</u></b>			
<b>T1 in [kN]</b>			
IDEA StatiCa	3920.00	3960.00	4640.00
Abaqus	3901.10	3947.22	4612.62
Comparison	100.5%	100.3%	100.6%
<b>T2<sub>y</sub> in [kN]</b>			
IDEA StatiCa	3840.00	3870.00	4470.00
Abaqus	3815.82	3859.21	4446.53
Comparison	100.6%	100.3%	100.5%
<b>T2<sub>z</sub> in [kN]</b>			
IDEA StatiCa	3650.00	3700.00	4230.00
Abaqus	3624.36	3674.44	4197.45
Comparison	100.7%	100.7%	100.8%
<b>T3<sub>y</sub> in [kN]</b>			
IDEA StatiCa	2580.00	2620.00	3000.00
Abaqus	2578.91	2605.91	2989.56
Comparison	100.0%	100.5%	100.3%
<b>T3<sub>z</sub> in [kN]</b>			
IDEA StatiCa	1150.00	1150.00	1150.00
Abaqus	1145.03	1146.21	1149.50
Comparison	100.4%	100.3%	100.0%
<b>T4<sub>y</sub> in [kNm]</b>			
IDEA StatiCa	1220.00	1232.00	1416.00
Abaqus	1209.00	1222.00	1402.01
Comparison	100.9%	100.8%	101.0%
<b>T4<sub>z</sub> in [kNm]</b>			
IDEA StatiCa	373.00	373.00	373.00
Abaqus	368.90	369.10	369.10
Comparison	101.1%	101.1%	101.1%



Table 8: LBA Results – IPE500

	Eigenvalue (EV)		
	EV1	EV2	EV3
<b><u>IPE500</u></b>			
<b>T1 in [kN]</b>			
IDEA StatiCa	6780.00	7200.00	9720.00
Abaqus	6752.43	7123.61	9500.34
Comparison	100.4%	101.1%	102.3%
<b>T2<sub>y</sub> in [kN]</b>			
IDEA StatiCa	6700.00	7100.00	9600.00
Abaqus	6711.60	7071.83	9405.83
Comparison	100.6%	100.4%	102.1%
<b>T2<sub>z</sub> in [kN]</b>			
IDEA StatiCa	6720.00	7080.00	9420.00
Abaqus	6703.95	7059.50	9395.84
Comparison	100.2%	100.3%	100.3%
<b>T3<sub>y</sub> in [kN]</b>			
IDEA StatiCa	5960.00	6200.00	8000.00
Abaqus	5939.74	6145.82	7876.32
Comparison	100.3%	100.9%	101.6%
<b>T3<sub>z</sub> in [kN]</b>			
IDEA StatiCa	3768.00	3788.00	3788.00
Abaqus	3737.90	3754.62	3759.72
Comparison	100.8%	100.9%	100.8%
<b>T4<sub>y</sub> in [kNm]</b>			
IDEA StatiCa	4808.00	4864.00	5952.00
Abaqus	4774.35	4831.90	5903.46
Comparison	100.7%	100.7%	100.8%
<b>T4<sub>z</sub> in [kNm]</b>			
IDEA StatiCa	1236.00	1236.00	1244.00
Abaqus	1227.90	1228.40	1233.70
Comparison	100.7%	100.6%	100.8%

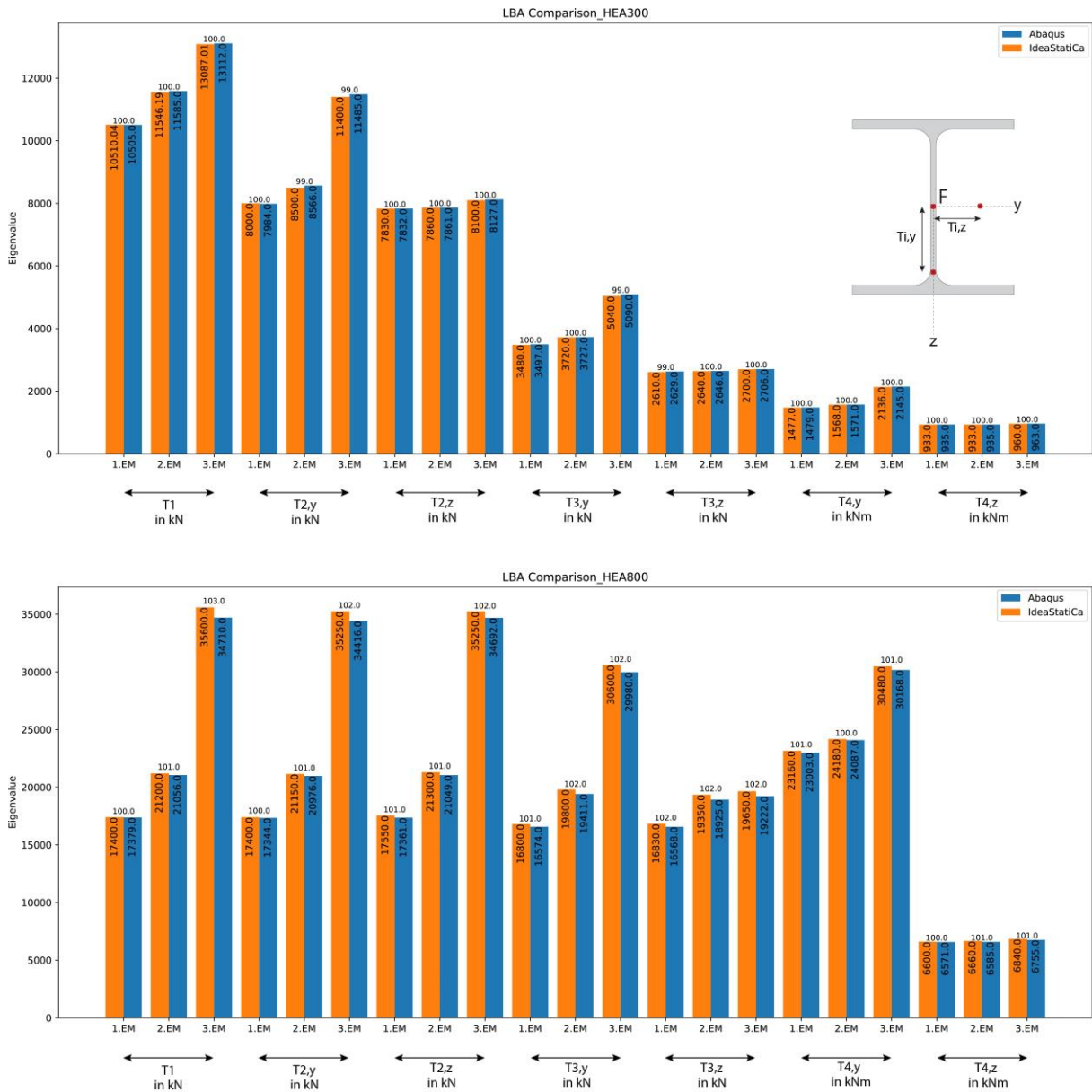


Figure 8: Comparison of LBA results for HEA300 and HEA800

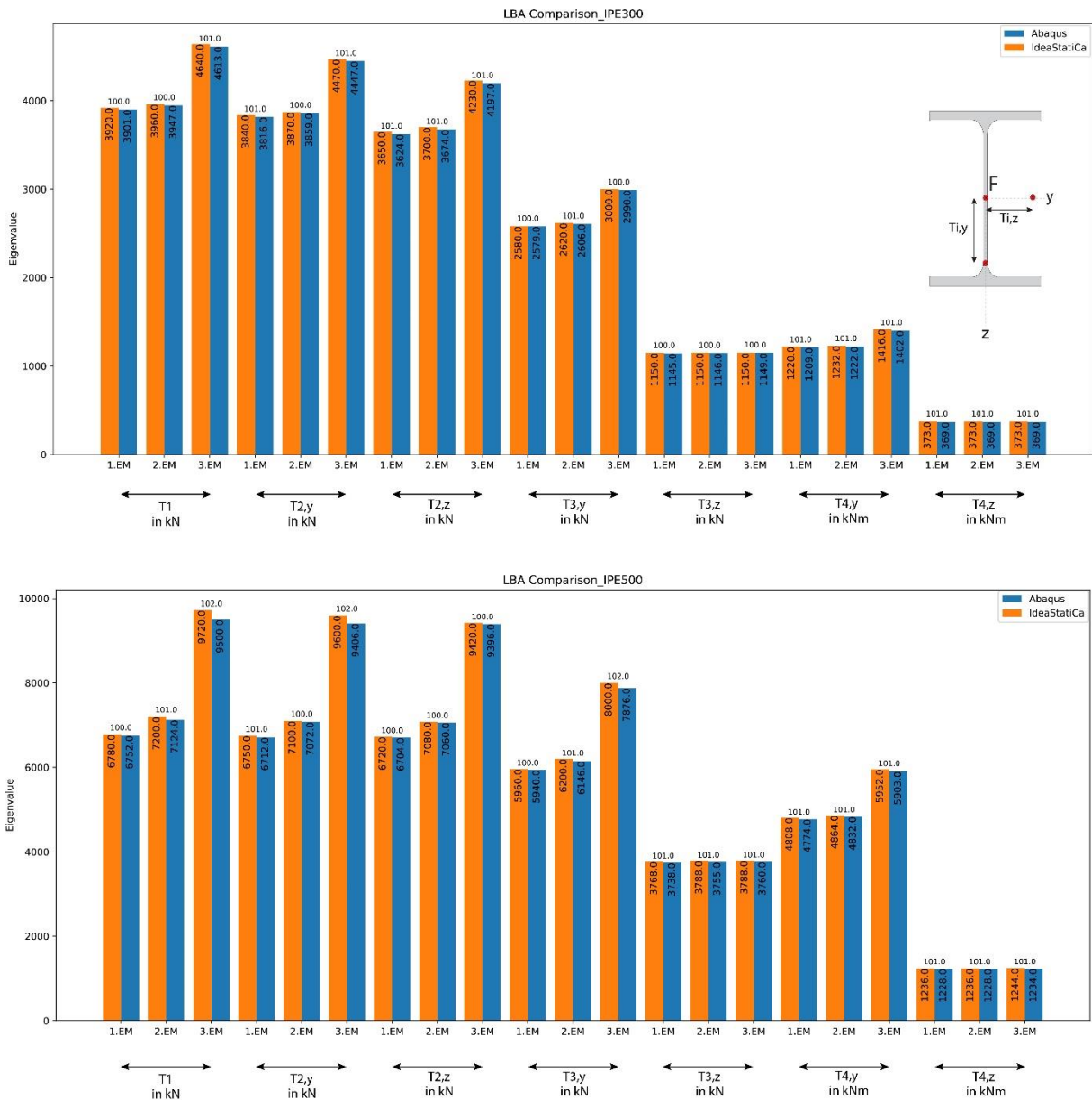


Figure 9: Comparison of LBA results for IPE300 and IPE500

The results of the LBA comparison are summarized in Tables 3 to 6 and additionally shown in Figure 4 and 5, respectively. The LBA comparison generally shows very small deviations between the results of IDEA StatiCa Member and Abaqus, for the three considered eigenvalues (EV1–EV3) related to the different load conditions from Table 1. A maximum difference of 3% can be identified for the HEA800 profile, load case T1, EV3 (s. Figure 4, bottom). However, all other results show significantly smaller differences between the bifurcation loads and are therefore well within the range of acceptance. It should be noted here that IDEA StatiCa Member provides in most cases a slightly higher linear buckling factor than Abaqus.

## 5.2. Comparison of the GMNIA Results:

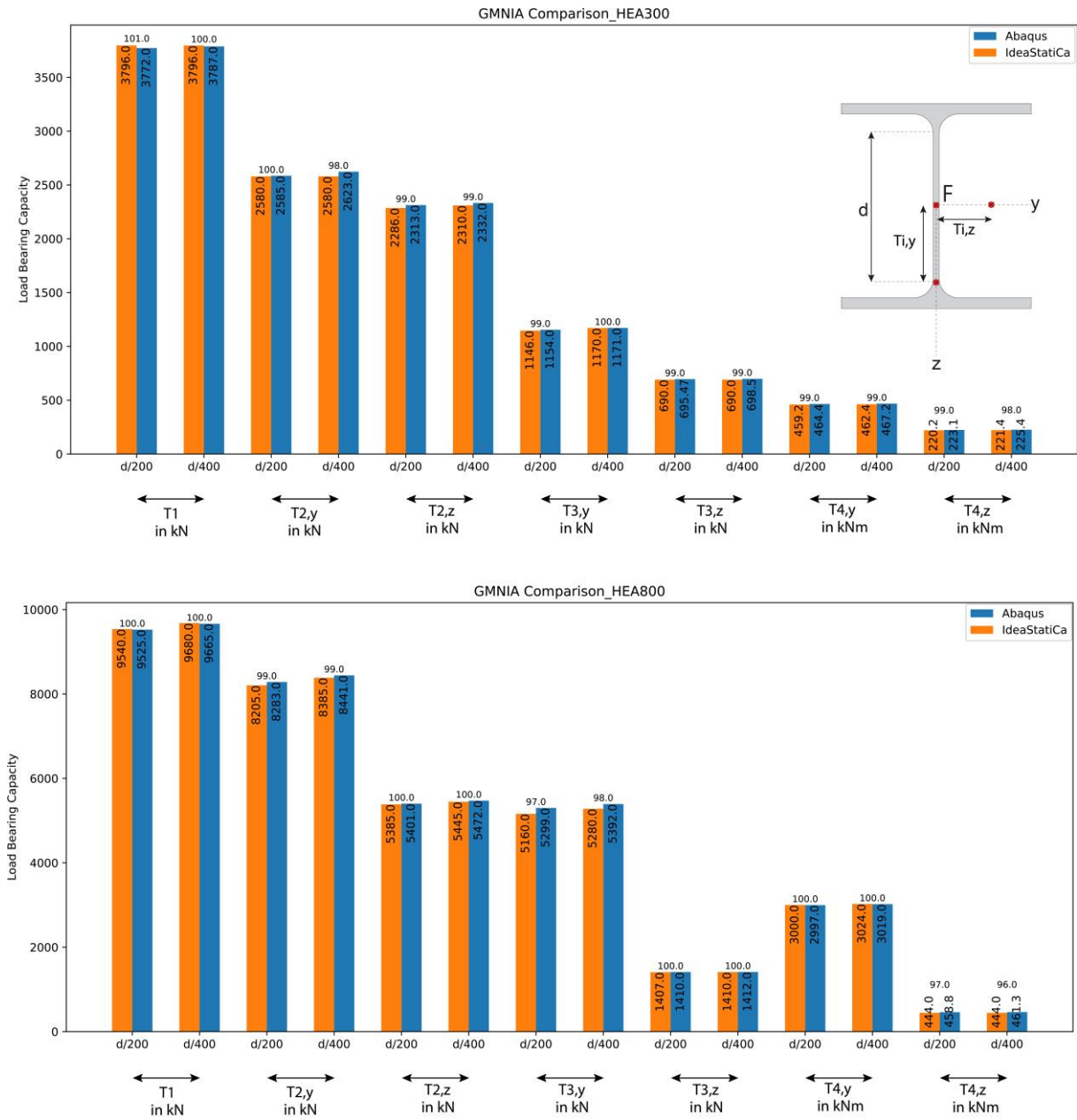


Figure 10: Comparison of GMNIA results for HEA300 and HEA800

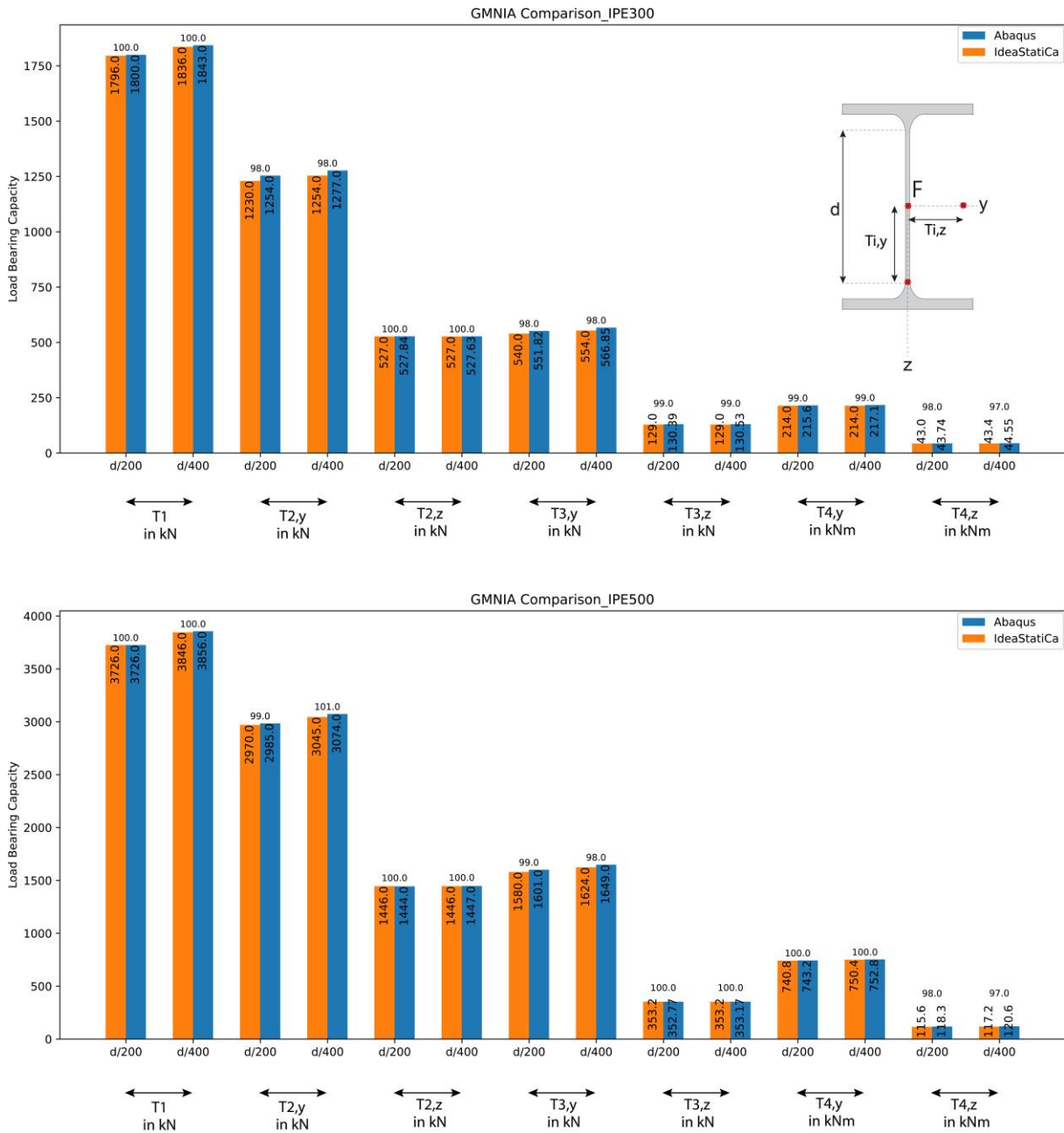


Figure 11: Comparison of GMNIA results for IPE300 and IPE500

The GMNIA results are summarized in Fig. 10 and 11, again for all load conditions displayed in Table 1. The resistance comparison between IDEA StatiCa Member and Abaqus generally shows only minor deviations of the achieved maximum loads for load combinations T1 to T3 with no greater deviation than 2%. With rising eccentricity a slight increase between the compared loads is detected with a maximum of 3% (s. Figure 7, bottom, load combination T4,z). The achieved loads, calculated by IDEA StatiCa Member are always slightly lower than the calculated loads in Abaqus. Again, this level of deviation is common and well between the range of acceptability.

## 6. Choice of eigenmode shapes for interactive cases of global + local buckling

The strength predictions based on GMNIA calculations can be strongly dependent on the choice of imperfection shapes, which are determined in advance by LBA analysis and the respective associated imperfection amplitudes. A common approach is to use the shape of the first eigenmode as the applied initial imperfection for subsequent GMNIA calculations. However, in important cases, this approach could neglect a possible interaction between local and global buckling, with significant consequences for the estimated load-bearing capacity. For this reason, it is important to ensure that *both* local and global imperfection shapes are included in the GMNIA calculations whenever an interaction between the two is detrimental. On the other hand, it may be both unnecessary and cumbersome to *always* consider both types of imperfection. For this reason, recommendations are developed in the following section based on examples and previous experience of the authors.

For the Abaqus [1] calculations carried out for this purpose and summarized in Fig.12, the amplitudes of the local and global imperfections were set to a constant value of  $d/200$ , in the case of the local amplitude and a length affine, buckling curve dependent global amplitude according to EN 1993-1-5 [4] and EN 1993-1-1 [2], respectively. Fig. 12 shows the results of GMNIA simulations for a centrally loaded, hot rolled HEA300 and IPE500 profile of steel grade S355 with varying member lengths for buckling about both axes  $z-z$  and  $y-y$ .

In each of the presented diagrams three different sets of GMNIA calculations were performed in order to obtain the load-bearing capacity using only the local eigenform (red dots), a combination of the local and global eigenforms (blue dots) and the global eigenform exclusively (green dots). The local capacity (red dots) is always represented through the local slenderness, which was estimated through LBA calculations and therefore remains almost at the same spot for different lengths. This forms an artificial "transition line" separating the "dominant" first eigenforms into local and global imperfection shapes. Therefore, all models with a calculated  $\alpha_{cr,glob} < \alpha_{cr,loc}$  will have a first eigenmode governed by global buckling, while all models with  $\alpha_{cr,glob} > \alpha_{cr,loc}$  have a local first eigenmode. The global capacity (green and blue dots), on the other hand, is represented through the global slenderness, again estimated through LBA calculations performed in advance.

Fig. 12 a and c shows the results for a hot-rolled HEA300 profile, for buckling about  $z-z$  and  $y-y$  axes. The corresponding  $\alpha_{cr,loc} = 2.50$  lies between the global and local limit values of  $\alpha_{lim,glob} = 25$  and  $\alpha_{lim,loc} = 2.20$ , derived respectively from the plateau values of the column buckling curves of EN 1993-1-1 [2] and the "Winter curve" for plate buckling (case of constant compression in a plate supported on all four sides). Due to the fact that  $\alpha_{cr,loc} > \alpha_{lim,loc}$  local effects do not have a significant influence on the overall behaviour of this thicker-walled section. This is confirmed by comparing the GMNIA results of the global capacity, using the overlaid global and local eigenforms and the GMNIA results using the global eigenform only, leading to a maximum difference of lower than 1.0% and the conclusion that local imperfections have a subordinate influence for the considered cross-section. On the other hand, local imperfections generally need to be taken into account in cases where  $\alpha_{cr,loc} < \alpha_{lim,loc}$ ; see Fig. 12 b and d.

Comparing the GMNIA results of the global capacity again, taking the superposition of global and local eigenmode as opposed to only the global eigenmode, will lead to significant differences. Neglecting the inclusion of local imperfections would lead to an overestimation of the maximum load by up to 7% for the investigated cases of buckling around both axes z-z and y-y, especially for shorter members. On the other hand, for shorter members it may be convenient and suitable to only account for local buckling in GMNIA design calculations.

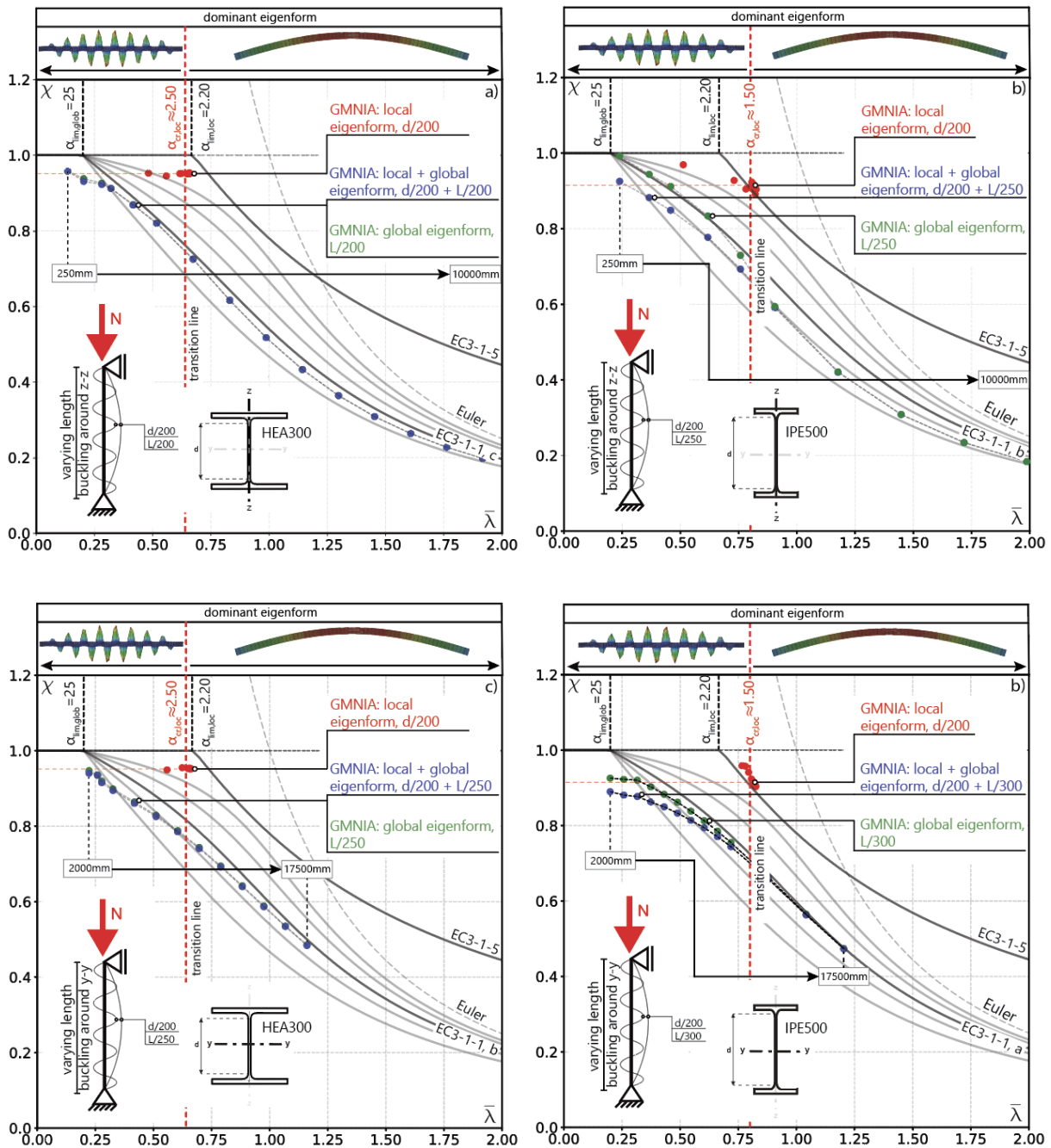


Figure 12: Impact of the choice and combination of the eigenforms on the buckling resistance a, b) buckling around z-z axis for an HEA300 and IPE500 profile; c, d) buckling around y-y axis for an HEA300 and IPE500 profile



The requirement to apply – or not – global imperfections may be formulated depending on the value of  $\alpha_{cr, glob}$  and its ratio to  $\alpha_{cr, loc}$  denominated as “ $f$ ” in the following (see Eq. 3).

$$f = \frac{\alpha_{cr, glob}}{\alpha_{cr, loc}} = \frac{\lambda_{loc}^2}{\lambda_{glob}^2} \quad (3)$$

One obvious limit case for which it is certainly appropriate to neglect the global imperfections is given for cases where  $\alpha_{cr, glob} \geq \alpha_{lim, glob}$  is fulfilled. This would be equivalent to a case where the compression member is so stocky that it comes to lie in the “plateau” of the global buckling curves of EN 1993-1-1 [2]. If the upper condition is not met, the relation described by factor  $f$  (see Eq. 3) may be checked and a limit factor may be used to ensure that, if the distance between the two  $\alpha_{cr}$ -values is high enough, the influence of global imperfections is small enough to be neglected. In these cases, GMNIA calculations may be performed considering only local imperfections, as these will determine the resistance entirely.

Based on experience and the theoretical considerations of the analytical buckling curves and their relative distance, it was possible to formulate the following, safe-sided recommendations. Therefore, whenever it becomes necessary to include local imperfections in GMNIA calculations (cases with  $\alpha_{cr, loc} < \alpha_{lim, loc}$ ), the simultaneous consideration of global imperfections may be neglected if factors  $f$  exceed the following limit values (valid for I-shaped sections):

- $f_{lim, a} = 3.50$  for I-shaped sections buckling curve a applies
- $f_{lim, b} = 4.50$  for I-shaped sections buckling curve b applies
- $f_{lim, c} = 6.00$  for I-shaped sections buckling curve c applies

The flowchart below provides a practice-oriented overview of the above-described decision criteria. The values of  $\alpha_{lim, loc}$  and  $\alpha_{lim, glob}$  are 2.2 and 25, respectively.

The following two examples shall explain the general workflow of the presented flowchart:

**Worked out Flow Chart Example 1 -  $\alpha_{cr, loc} \geq \alpha_{lim, loc}$  (Fig. 12 a, c):**

In the first considered case  $\alpha_{cr, loc} > \alpha_{lim, loc}$ , therefore high enough that it comes to lie in the plateau of the nominal curve of EN 1993-1-5 [4] (Winter curve), meaning that the relative local slenderness of the profile is small without having a significant influence on the overall behaviour of the member. This can also be identified in Fig. 12 a) and c), as no difference between the estimated results of “**GMNIA with global imperfections**” and “**GMNIA with local + global imperfections**” is visible/detected within the numerical simulations. Depending on the global slenderness, respectively the value of  $\alpha_{cr, glob}$ , two triggering conditions are interesting for the further choice of the global imperfection. If  $\alpha_{cr, glob} < \alpha_{lim, glob} = 25$  a global imperfection has to be applied according to EN 1993-1-1 [2], meaning that the profile is prone to global instabilities. If the condition  $\alpha_{cr, glob} \geq \alpha_{lim, glob} = 25$  is met, meaning that the profile is so short that it comes to lie in the plateau of the global buckling curve, no further imperfections need to be applied (see Fig. 12 a) for  $L = 250$  mm).



**Worked out Flow Chart Example 2 -  $\alpha_{cr,loc} \leq \alpha_{lim,loc}$  (Fig. 12 b, d):**

In this particular case  $\alpha_{cr,loc}$  is lower than the limit value of  $\alpha_{lim,loc} = 2.2$ , according to EN 1993-1-5 [4], and therefore local imperfections have a dominant influence on the load-bearing capacity except for the cases where  $\alpha_{cr,glob} \leq \alpha_{cr,loc}$ , meaning that the length of the profile and its associated global imperfection amplitude are dominating the overall interactive behaviour. The horizontal red dotted line, throughout all diagrams of Fig. 12, indicates this transition area. If this case applies, the bespoke procedure of “Flow Chart Example 1” must be carried out, since only the choice of whether the global imperfection has to be used or not, must be considered. In cases where  $\alpha_{cr,glob} > \alpha_{cr,loc}$ , two further possible conditions must be investigated. For very short profiles where  $\alpha_{cr,glob} \geq \alpha_{lim,glob}$  only local imperfections need to be taken into account, since the profile has on the one hand high local slenderness but at the same time very low global slenderness. Additionally, a combination of local and global imperfections must be considered if the value  $f_{lim} = \alpha_{cr,glob} / \alpha_{cr,loc}$  (according to the global buckling curve a, b or c) is not reached.

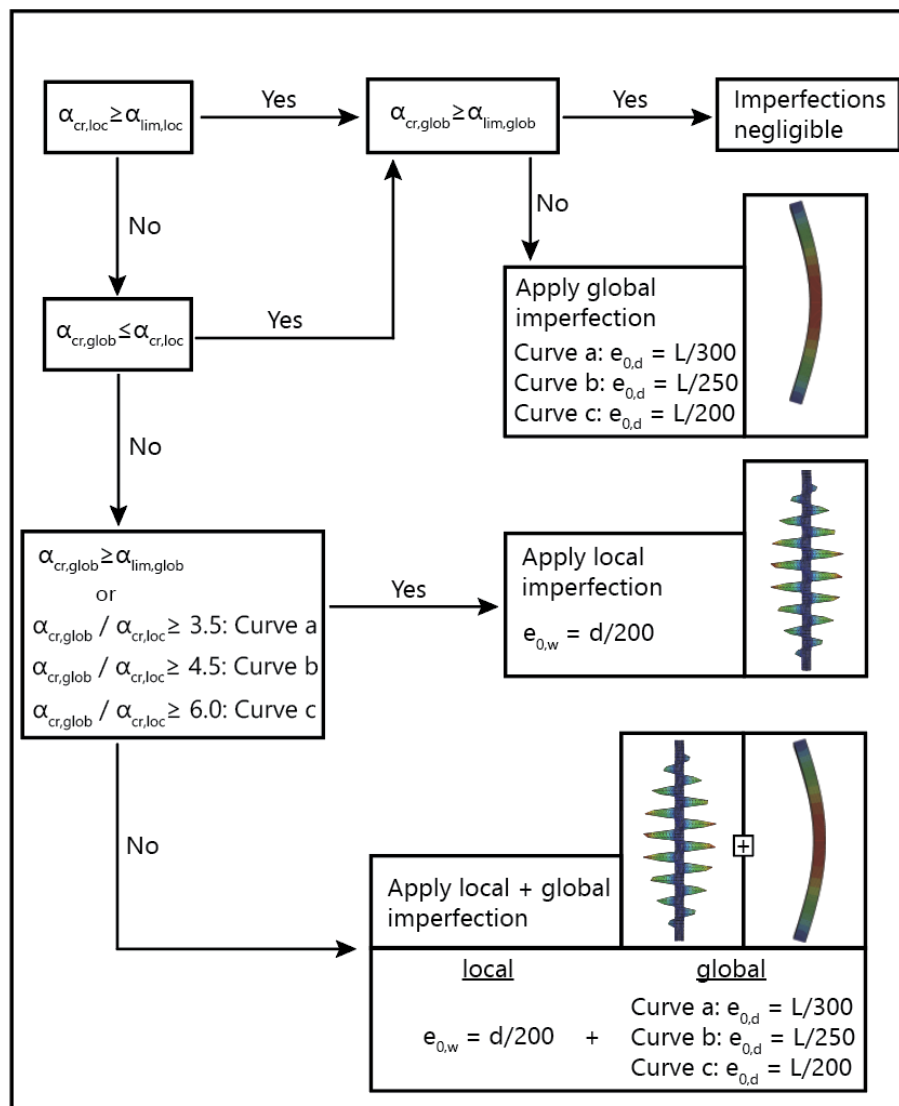


Figure 13: Flow chart to determine the applied imperfections

## 7. Conclusions

The comparison between the calculations in the IDEA StatiCa Member software and the FEM program Abaqus showed generally small deviations in the LBA as well as GMNIA results with a maximum difference of 3% in individual cases. This level of deviation is common and well between the range of acceptability.

Investigations on the choice of local and global imperfection amplitudes – according to code provision of EN 1993-1-1 [2], prEN 1993-1-1 [3] and EN 1993-1-5 [4] – lead to the following conclusions.

- In terms of local buckling the imperfection amplitude of  $d/200$  showed a good agreement with the EN 1993-1-5 [4] “Winter curve” for plate buckling (case of constant compression in a plate supported on all four sides and in constant compression).
- Based on the calculations in section 4.2 a length proportional approach according to EN 1993-1-1 [2] is sufficient and safe-sided when using the elastic design approach for the evaluation of imperfection amplitudes. The same can be stated for the new formulation of the imperfection amplitude (see Eq. 1) regarding prEN1993-1-1 [3]. It should be noted that  $\beta$ , the new reference bow imperfection (see Tab. 2), is not only dependent on the design approach but also the buckling axis “y-y” or “z-z”.
- When using the slenderness affine imperfection amplitudes according to EN 1993-1-1 [2] and prEN 1993-1-1 [3], it is recommended to use the plastic resistance. This approach requires that the magnitude of the relative slenderness is determined beforehand. Additionally, the calculating of an imperfection amplitude for buckling around “y-y” or “z-z” axis must consider the axis-related section modulus  $W_{pl,y}$  or  $W_{pl,z}$ .

Additional investigations were carried out to provide decision support, whether an interaction of local and global imperfections is required or not. Therefore, a safe-sided recommendation was formulated, introducing limit values ( $f_{lim}$ ), which are derived from the relative distance of the analytical buckling curves of EN 1993-1-1 [2] and EN 1993-1-5 [4]. Whenever these limits are exceeded by the calculated factors  $f$  (see Eq. 3), global imperfections may be neglected in cases with  $\alpha_{cr,loc} < \alpha_{lim,loc}$  for the consideration of I-shaped hot rolled and welded cross-sections. It shall be noted that Annex C of EN 1993-1-5 [4], as well as prEN 1993-1-14 [9] (Design by FEM), make use of the “70%-rule” for the combination of imperfection modes and amplitudes. This rule postulates that *two* GMNIA calculations should be carried out when local + global interactive buckling may be dominant: one with 100% + 70% of the maximum specified amplitude in either case. In this report, however, we recommend avoiding this double calculation by using the amplitudes given in section 4.2 for global buckling and the amplitude of  $d/200$  (see section 4.1) for local buckling. This is sufficiently accurate and safe-sided for all cases that require a combined consideration of imperfections according to the presented flowchart in section 6, Fig. 13.

## 8. Literature and References

- [1] Abaqus. Reference manual, version 6.16. Simulia, Dassault Systéms, France, 2016.
- [2] EN 1993-1-1. Eurocode 3. Design of steel structures – Part 1-1: General rules and rules for buildings. *CEN – European Committee for Standardization*. Brussels, 2005.
- [3] prEN 1993-1-1. Eurocode 3. Design of steel structures – Part 1-1: General rules and rules for buildings. *CEN – European Committee for Standardization*. Brussels, 2019.
- [4] EN 1993-1-5. Eurocode 3. Design of steel structures – Part 1-5: Plated structural elements. *CEN – European Committee for Standardization*. Brussels, 2006.
- [5] Taras, A. (2011) Contribution to the Development of Consistent Stability Design Rules for Steel Members. Dissertation, Institut für Stahlbau und Flächentragwerke, TU Graz, Heft 16, Graz.
- [6] Kindmann, R.; Kraus, M. (2019) FE-Berechnung mit Fließzonen für Tragfähigkeitsnachweise nach DIN EN 1993-1-1, Vereinfachte Berechnungsmethode für stabilitätsgefährdete Bauteile. *Stahlbau* 88, H. 4, S. 354-362.
- [7] Trahair, N. (1993) Flexural-Torsional Buckling of Structures. *New Directions in Civil Engineering*, London.
- [8] Beer, H.; Schulz, G. (1970) Bases Théoriques des Courbes Européennes de Flambement. *Constr. Métallique*, Vol. 3, pp. 37-57.
- [9] prEN 1993-1-14. Eurocode 3: Design of steel structures — Part 1-14: Design assisted by finite element analysis. *CEN – European Committee for Standardization*. Brussels, 2021.